Structure and Gas Parameters of Plume Expiring into Vacuum from Four Nozzles Located Around the Space Vehicle Case

Yury I. Gerasimov*, Andrey N. Krylov*, Vyacheslav N. Yarygin†

* - *Korolev Rocket and Space Corporation ENERGIA, Korolev, Russia*
† - *Kutateladze Institute of Thermophysics SB RAS, Novosibirsk, Russia*

Abstract. Results of experimental and numerical researches of gas parameters in an interaction zone of four jets escaping from rocket engines located around the case are presented.

INTRODUCTION

Docking and undocking of space vehicles (SV) often involves simultaneous operation of four rocket reactive control system (RCS) thrusters located around the active SV case. Such a scheme of jets expansion has been implemented in the project of the SV "Apollo" (the mutual position of “Apollo” and SV “Soyuz” in joint flight (1975) is shown in Fig. 1a) and in a number of current Russian spacecraft projects. There is a complex shock structure behind which local values of density and pressure of the gas increase, arising at interaction of jets with each other and with the SV case in a compound jet flow field. The greatest intensification of flow field parameters is observed in the interaction zone of four jets where the second passive SV is located. The main parameters of thruster installation around the SV case are shown in Fig. 1b.

The structure and flow field parameters of such a compound jet were investigated in a series of simulation and numerical experiments. Simulation experiments were performed in a vacuum chamber of IT SB RAS [1] in a series of eight experiments. Numerical experiments were conducted with an “AeroShape-3D” program [2].

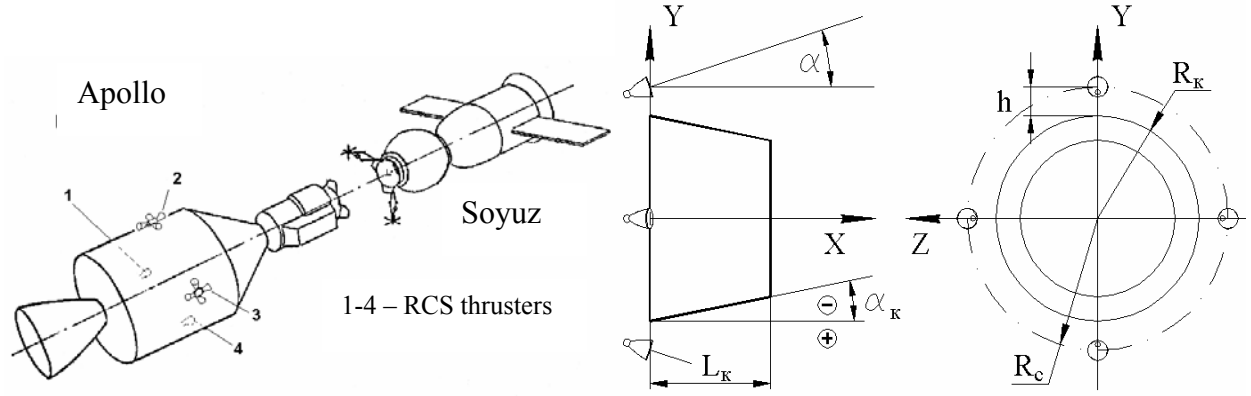

(a) (b)

FIGURE 1. Thruster installation around the SV case.

SIMULATION EXPERIMENTS

The following geometric parameters of the models (Table 1) were varied in experiments: nozzle expansion $\overline{F}$ =9, 20, and 30 (the nozzle-throat diameter was d_* =2r_* ≈0.5 mm), R_k/h =3.3 and 14, L_k/r_a =14, 24, and 35, and α_k from -8^0 up to $+10^0$. The angle of nozzle inclination to the longitudinal axis α was 15^0 at the height of nozzle installation above the case h/r_a=3. The modeling gases were N_2 and CO_2, and the Reynolds numbers Re_* were within the range from 0.5×10^5 to 0.9×10^5.

TABLE 1. Parameters of modeling researches.

Model number	Gas	$\overline{F}$	$R_к/h$	$L_к/r_a$	$\alpha_к$
1.1	CO_2	30	3.3	23.8	0
1.2	N_2	20	14	35	0
1.5	N_2	9	14	25	0
2.1	N_2	9	14	25	8^0
2.2	N_2	9	14	25	-7^0
2.3	CO_2	30	3.3	23.8	8^0
2.4	CO_2	30	3.3	23.8	-7^0
2.5	N_2	20	14	14	10^0

Using the electron beam method, the flow field structure was visualized (Fig. 2), and the local density distributions were measured in jets behind the case along the longitudinal axis *X* of the model (Fig. 3a) and in the cross sections *X*=*const* and *Y*=0 (Fig. 3b, 3c).

The following flow field structure was formed (Fig. 4). Above the case 4, shocks S_1 are formed. The neighboring jets interact with each other with formation of shocks S_2 in the flow field zones *3*.

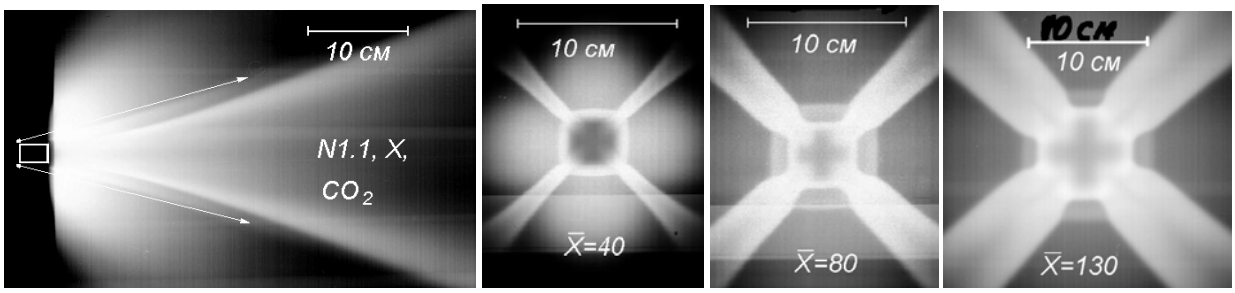

FIGURE 2. Results of flow field wave structure visualization in an experiment with model 1.1.

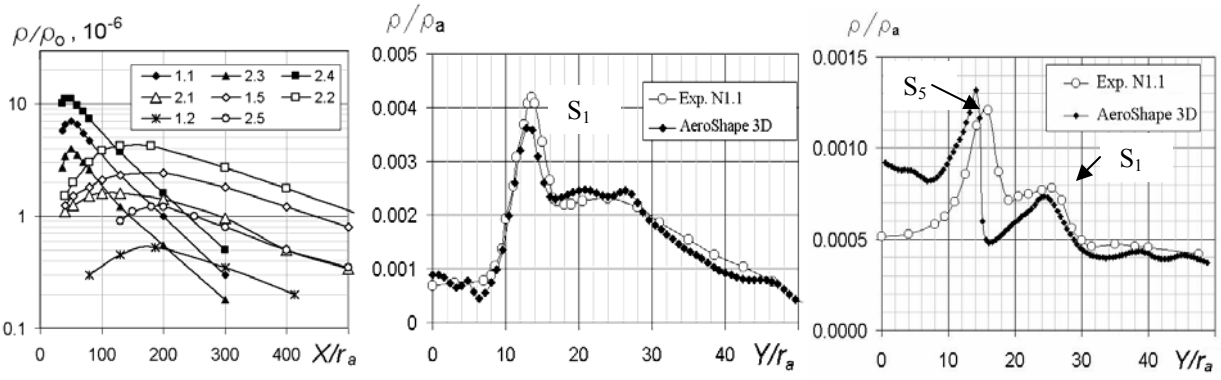

(a) (b) (c)

FIGURE 3. Results of experiments

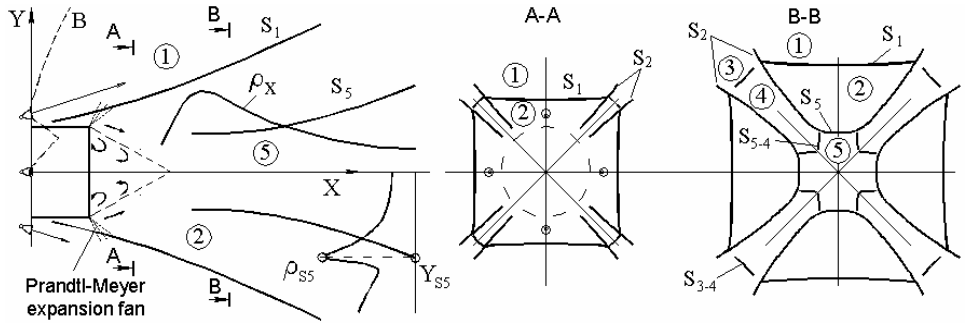

FIGURE 4. Flow field structure of a compound jet behind the SV cut.

In the next jet interaction zones located inside the S_1 shock front contours, there arise zones *4*. The next jet boundariess *B* lead to formation of the central area of the field isolated from the external flow. Behind the cut of the SV case, a circulating zone of backflows is formed, and an interference zone 5 is formed in the wake. The boundariess of zone 5 are the shock waves S_5 formed owing to interference of the shocks S_2 in the planes Y=0 and Z=0, and the shocks $S_{5\text{-}4}$ separating zones *4* and *5*.

The gas density distribution along the longitudinal axis of the configuration has a clearly expressed maximum (Fig. 3a), and the values of density in the shock waves S_5 are two to three times higher than the level observed in undisturbed jet zones.

The concept of a characteristic vacuum-jet angle $\theta_+ = arctg\sqrt{(1-\bar{J})/\bar{J}}$ determined by the value of the relative impulse of the jet $\bar{J} = J_a/(G_* \cdot V_{\max})$ [3] was used to analyze the simulation and numerical experiments. In this model, the distribution of gas density in an undisturbed plume $(\bar{r} = r/r_a > 10)$ is

$$\frac{\rho}{\rho_0} = \frac{0.21 \cdot (\gamma - 1)^{0.5}}{\bar{F} \cdot \bar{r}^2 \cdot \theta_+^2} \exp(-0.5 \cdot \bar{\theta}^2) \qquad (1)$$

where $\bar{\theta} = \theta/\theta_+$, *r,* and θ are the coordinates of the polar system.

For modeling CO_2 and N_2 jets, the values of the characteristic angles θ_+ were determined experimentally. The CO_2 ($\bar{F}$ =30) and N_2 ($\bar{F}$ =9) jets had identical values of the characteristic angles $\theta_+ \sim 22^0$. For N_2 jets ($\bar{F}$ =20), the angle was $\theta_+ \sim 18^0$.

NUMERICAL EXPERIMENTS

The simulation researches involved wide ranges of the parameters $R_к/h$, $L_к/R_к$, and $\alpha_к$; the limited number of experiments, however, did not allow us to find the basic laws and dependences defining the sizes of boundariess and the density distribution in the interference field of four jets field (zone *5*). The question of the change in velocity of the gas passing through a system of shock waves was also left outside the experimental researches. Unresolved issues were considered in numerical experiments.

The "AeroShape 3D" program has a restriction from below on static pressure in the computational domain (minimum pressure of ~10 Pa). For this reason, the calculations were performed for nozzle-exit gas pressures overestimated by three orders. Therefore, the first test computations were performed for configurations similar in geometry and characteristic jet expansion angles to those investigated in experiments at IT SB RAS.

The results of testing the calculation method are plotted in Figs. 3a and 3b, which show the calculated and experimental data on gas density in the cross-sections $\bar{X} = 40$ and $\bar{X} = 80$ in the plane *Z*=0 for model No.1.1. In the cross section $\bar{X} = 40$, the positions of flow area boundariess (shock waves) and the density distributions obtained by calculations agree well with the experimental data. At $\bar{X} = 80$, the gas density in shock waves in modeling and numerical cases are in good agreement. At the axis of the configuration, however, the density values in this cross section appear to be overestimated approximately by 40-60 %, which is obviously related to the influence of viscosity effects in simulation conditions.

The calculations results actually reflect the picture of a perfect gas flow. They were used to find the positions of the boundariess and the density distributions in the interference field of four jets (zone *5*).

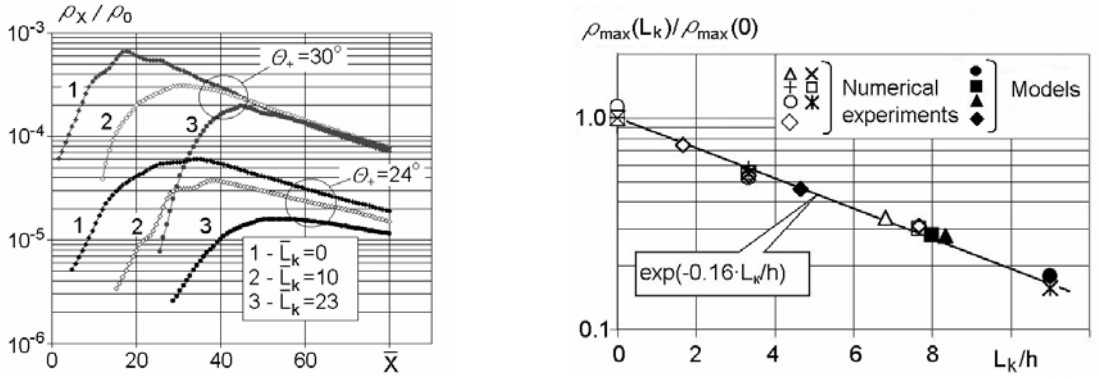

(a) (b)

FIGURE 5. Results of numerical experiments: a) change in gas density on the *X* axis depending on the value of the characteristic angles θ_+ and case lengths, b) change in the maximum values of gas density with increasing case length.

Fifteen numerical experiments were performed, the major part of them (10) being conducted to determine the dependence of the distribution of flow parameters in zone *5* on conditions of jet expansion by characteristic angles θ_+ (ranging from 20 to 30^0) and on the change in the case length ($\bar{L}_\kappa$=0-23) at R_κ / h=3.33, 6.3, and 10. Four experiments were performed for the nozzle installation angle α=0 for different values of the parameter R_κ / h. The calculations results for R_κ / h=3.33 and α=15^0 (Fig. 5a) show the general character of gas density on the *X* axis of the configuration. An increase in the case length reduces the gas density on the jet axes, and the position $X_{\max}$ of the gas density maximum $\rho_{\max}$ is shifted toward higher *X* values. A decrease in the jet field characteristic angles θ_+ leads to a decrease in density.

The maximum values of gas density with increasing case length are approximated by the dependence (Fig. 5b)

$$\rho_{\max}(L_\kappa) / \rho_{\max}(0) = \exp(-0.16 \cdot (L_\kappa / h)) \qquad (2)$$

If the case is absent, the angular position of the density maximum on the configuration axis relative to the nozzle axes is determined by the dependence $\theta_{\max} \approx \theta_+(1.2 + 2 \cdot \bar{\varphi})$, where $\bar{\varphi} = \varphi / (3\theta_+ \cdot \bar{J}^{0.5})$ is a dimensionless parameter determining the position of the interaction plane (or planes) relative to the jet flow field [3]. The case surface generates disturbances, both in the single jet field and in the jet interaction zone. It is convenient to use the coordinate of the gas density maximum position in the zone of interaction of adjacent jets X_{m2} ($L_\kappa = 0$) to determine the gas density maximum position on the configuration axis (X_{m5}). The value of X_{m2} is determined by the dependence $\bar{\theta}_{m\rho} = 1.1 + 2 \cdot \bar{\varphi}$ obtained by analyzing a series of similar numerical experiments for a case of interaction of two jets. These parameters varied within 20 to 30^0 (θ_+) and 0 to 0.25 ($\bar{\varphi}$). A generalized dependence was obtained (Fig.6a), which reflects the influence of the case length on the position of the gas density maximum on the configuration axis in an obvious manner $(X_{m5} - K_R \cdot X_{m2}) / R_c = f(L_\kappa / R_\kappa)$. The influence of the cross-sectional size of the case in this dependence is expressed by the values of K_R. For R_κ / h=3.33, this factor has a value equal to ~0.9 and linearly increases with increasing relative case size (Fig. 6b):

$$K_R = 0.59(1 + 0.15(R_k / h)). \qquad (3)$$

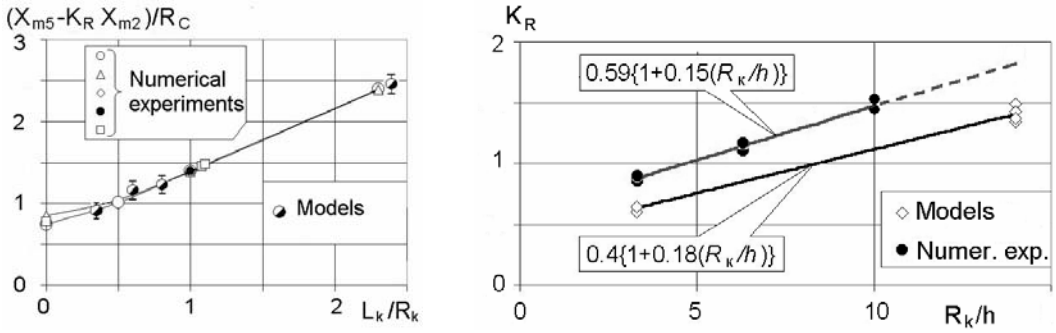

(a) (b)

FIGURE 6. Results of the modeling and numerical experiments: maximum gas density position depending on case parameter.

GENERALIZATION OF MODELING EXPERIMENT RESULTS

Combined consideration of the gas density distributions in cross sections $\rho(Y)$ and along the longitudinal axis of the model $\rho(X)$ showed that the shock wave S_5 emerges in the cross-section located near the point of the gas density maximum on the axis *X*. For planes of symmetry *Z*=0 or *Y*=0, the results of experiments on the spatial position of the front of the shock wave S_5 are described by uniform reduction of the coordinates *X* and Y_{S5} as

$$\overline{X}_n = (X - X_{m5}) / R_c \qquad \overline{Y}_n = Y_{S5} / R_c \tag{4}$$

where X_{m5} is the coordinate of the maximum density position on the longitudinal axis, which is defined (as is shown in Fig. 6a) using the dependence $K_R = 0.4(1 + 0.18(R_k / h))$ obtained from the results of modeling experiments (Fig.6b). In this form, the experimental data are shown in Fig. 7a.

The generalized function of the gas density change along the longitudinal axis of the model (according to Fig.3a) is shown in Fig. 7c. As in the description of the shock-wave form, the values of the longitudinal coordinate *X* are brought to the form $\overline{X}_n$ (4). The value of the parameter $\overline{\rho}_{X \cdot n}$ in Fig. 7c is defined by the relation

$$\overline{\rho}_{X \cdot n} = \rho_X / (\rho_{\max}(L_k) \cdot K_\alpha), \tag{5}$$

where the values of $\rho_{\max}(L_\kappa)$ are calculated by formula (2) in which the experimental data are extrapolated at $L_\kappa = 0$, and the value of $\rho_{\max}(0)$ is defined as $\rho_{\max}(0) / \rho_1 \approx 13 \cdot \sin \psi_m$. Here ρ_1 is the value of gas density in the single free jet flow field at the location of $\rho_{\max}(0)$, and ψ_m is the angle, as is shown in Fig. 7b. The factor K_α in (5) allows for the change of the model case inclination angle α_κ to the model axis. Generalization of data is brought to the formal form using the following formula for K_α : $K_\alpha = 1 + 3.8 \cdot \tan \alpha_\kappa$.

The relation of the density of the shock wave S_5 to its value on the axis *X* grows as the value of $\overline{X}_n$ increases from $\rho_{S5} / \rho_X \approx 2.3 \pm 0.3$ at the point of shock formation ($\overline{X}_n \sim 0$) to 3±0.3 in the far flow field, as a linear dependence: $\rho_{S5} / \rho_X = 2.25 + 0.032 \cdot \overline{X}_n$.

The data on gas-density distributions in the field zone 5 along the *Y* (or *Z*) axis are described, with an error smaller than 15 %, by functions that also include the parameter $\overline{X}_n$. The density distribution in the vicinity of the front of the shock wave S_5 ($Y / Y_{S5} = 0.6 \div 1.0$) is described by dependence

$$(\rho_5 - \rho_X) / (\rho_{S5} - \rho_X) = (1 - A_X) \cdot (Y / Y_{S5}) + A_X \cdot (Y / Y_{S5})^3 \tag{6}$$

where the value of the factor A_X is defined by the formula $A_X = 1.25 - 0.06 \cdot \overline{X}_n$.

In zone 5, near the axis *X* ($Y / Y_{S5} = 0 \div 0.6$), the change in density $(\rho_5 - \rho_X) / (\rho_{S5} - \rho_X)$ is described by a linear dependence.

The results of the analysis presented in the form of generalized dependences in formulas and in figures shown above approximate experimental data on the gas-density change in zone 5 (in symmetry planes Z=0 and Y=0) with a total error of ~25 %.

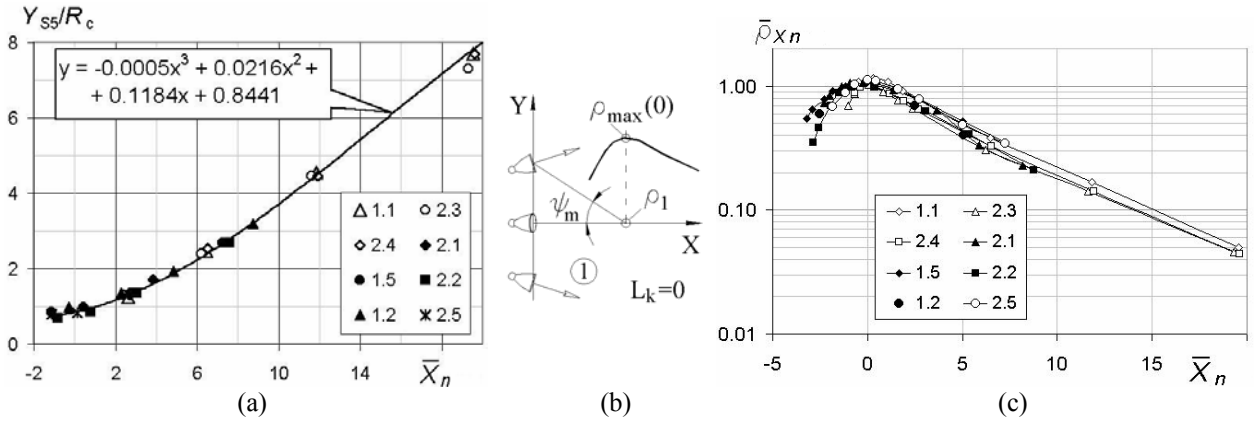

(a) (b) (c)

FIGURE 7. Generalization of modeling experiment results on the position of the front of the shock wave S_5 (a) and the change in gas density along the longitudinal axis of the configuration (c).

RESULTS OF NUMERICAL RESEARCHES OF CHANGES IN GAS VELOCITY

Zone 2. It follows from the calculation results that the decrease in gas velocity behind the shock wave S_1 relative to gas velocity in the free jet is less than 2 %. It is demonstrated in Fig. 8 which shows the results of a numerical experiment that simulated the condition of experiment 1.1. The data presented also demonstrate that the gas velocity in zone 2 equals V_{max} within ~5%.

Zone 5. The results of numerical experiments on gas velocity in the front of the shock wave S_5 (Y_{S5} point of gas density maximum) are described within 5 % by functions that also include the parameter $\overline{X}_n$ (3). The change in gas velocity at the maximum density point is shown in Fig. 9a as a function of the longitudinal coordinate $\overline{X}_n$. In the zone of the density maximum location ($\overline{X}_n$ =0), the gas velocity is 80±5% of V_{max}.

In the central interference zone (behind the shock wave S_5), the gas impulse $\rho \cdot V$ was considered for generalization of results. It allowed us to estimate the mismatch in calculated and experimental density values near the axis of the configuration *X,* which was noted in Fig. 3c for the far flow field. The results of numerical experiments for models with $\overline{L}_\kappa > 5$ lie in the hatched zone in Fig. 9b.

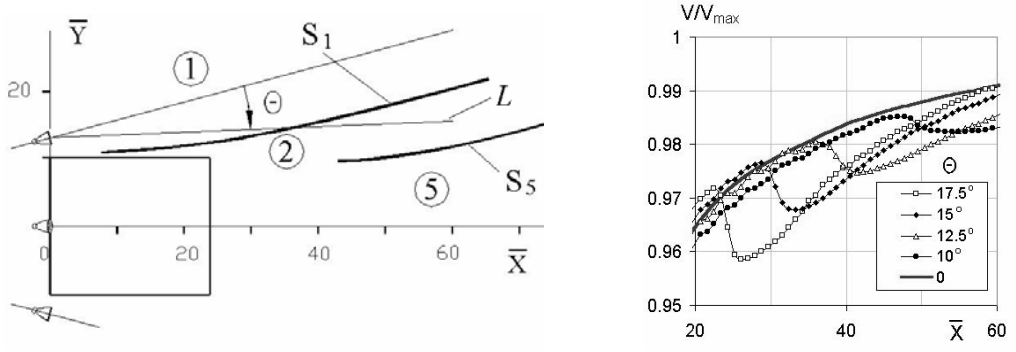

(a) (b)

FIGURE 8. Results of numerical experiments: change in gas velocity in zones *1* and *2* along the lines $L(\theta)$ versus the $\overline{X}$ coordinate (modeling experiment 1.1).

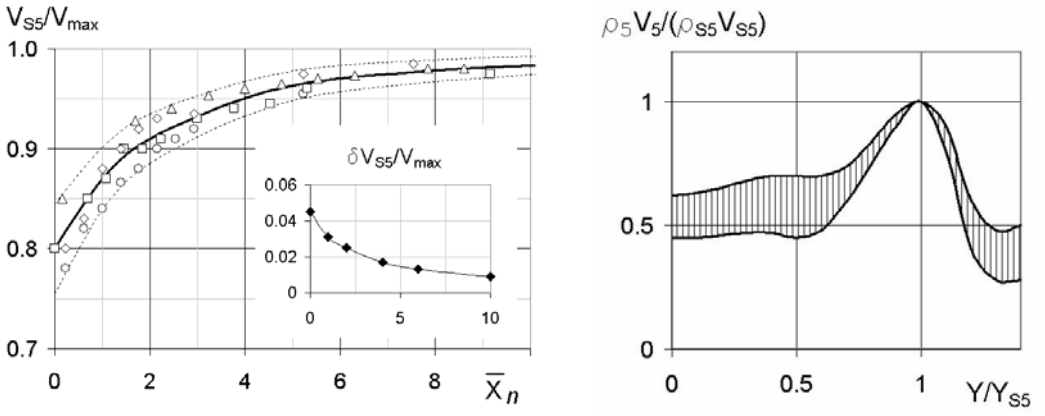

(a) (b)

FIGURE 9. Changes in gas velocity in the front of the shock wave S_5 (a) and gas impulse $\rho \cdot V$ in zone *5* (b).

REFERENCES

1. Yu.I. Gerasimov, S.A. Palopezhentsev, V.N. Yarygin, in *Proc. of VI All-Union Conference on Rarefied Gas Dynamics,* Novosibirsk, 1980, pp. 132-137.
2. V.N. Gavriliouk, A.V. Lipatnikov, A.N. Kozlyaev, E.V. Odintsov et al., "Computation modeling of the combustion problems with the use of "AeroShape-3D" Numerical Technique," *ISTS 94-d-27, 1994*.
3. Yu.I. Gerasimov, *Izvestiya Akademii Nauk SSSR, Mekh. Zhidk. Gaza,* No.2, 169-173 (1981).